Rearranged Coprime Array to Increase Degrees of Freedom and Reduce Mutual Coupling

Zhe Fu, Pascal Chargé, Yide Wang

Rearranged Coprime Array to Increase Degrees of Freedom and Reduce Mutual Coupling

Zhe Fu, Pascal Chargé, Yide Wang

Abstract

Coprime array for direction of arrivals finding has attracted increasing interest since it can provide enhanced degrees of freedom. However, due to the holes in the difference coarray, the available information is not fully exploited. In this paper, we propose a rearranged coprime array configuration to fill the holes in the coprime difference coarray. The proposed new array allows filling the holes and reducing the mutual coupling effect at the same time. We classify all the holes in a holes-triangle as a design guideline for the proposed rearranged coprime array. Few redundant sensors of the generalized coprime array are rearranged at sparse positions, which are determined by the position of holes. By doing so, the consecutive part of the conventional coprime difference coarray can be significantly increased. Meanwhile, the mutual coupling can also be dramatically reduced because the redundant sensors are relocated at remote positions. Simulation results verify the superiority of the proposed array compared with other sparse arrays.

Keywords: Rearranged coprime array, holes filling, degrees of freedom, mutual coupling.

1. INTRODUCTION

Array signal processing plays an important role in many applications, such as radar, sonar, navigation, wireless communications [1, 2, 3, 4]. Data measured from array sensors allow us to extract signal features, such as direction-of-arrival (DOA), frequency, and range. Traditionally, the most commonly used array structure is the uniform linear array (ULA), whose inter-element spacing is no more than half of the wavelength of incoming signals. Therefore, the array aperture of the traditional ULA relies on the number of sensors. In addition, due to the closely located sensors, the mutual coupling effect can significantly degrade the estimation performance.

Several sparse array structures are proposed to achieve higher degrees of freedom (DOFs) [5, 6, 7, 8] such that more sources than physical sensors can be detected. This is achieved by vectorizing the covariance matrix of the received signal and selecting the corresponding elements in the covariance matrix to construct a difference coarray [9, 10]. One of the most well known sparse arrays is the minimum redundancy array (MRA) [7], which aims to maximize the number of consecutive virtual sensors (holes-free) in the difference coarray for a given number of physical sensors. However, MRA does not have a closed-form expression for the array geometry. MRA geometries with less than 20 sensors [11] have been found by combinatorial search. It would be difficult to design a suitable MRA with a higher number of sensors. Minimum hole array (MHA) [12] also has this drawback which limits their application in practice.

The recently proposed nested array [8] and coprime array [13] can provide closed-form array geometry compared to MRA and MHA. But the classical coprime array has holes in its difference coarray [14, 15], and the mutual coupling effect is not negligible in the nested array [16, 17] because some sensors are densely distributed with a half wavelength inter-element spacing. The super nested array (SNA) is then designed to reduce the mutual coupling effect [18, 19] while keeping the main advantages of the nested array, such as, closed-form of sensor locations and hole free difference coarray. Another array configuration based on the nested array is the augmented nested array (ANA) [20]. ANA can increase the DOFs and reduce the mutual coupling in four different ways. However, the mutual coupling could increase when the number of sensors becomes large [21] for ANAI-1 and ANAI-2 (denoted as ANA1 and ANA2 in the following), while

the other two ANA arrays have to meet complicated conditions such that no holes occur in the difference coarray.

Since the classical coprime array [22] has holes in its difference coarray when the coarray MUltiple SIgnal Classification (MUSIC) [23] method or other subspace based methods are applied to the difference coarray, the discontinuous part cannot be used. This leads to some loss of DOFs. To enlarge the consecutive part, one sub-array can be increased from M sensors to $2M$ sensors [24] such that the consecutive part could be increased from $[-(M+N-1),(M+N-1)]$ to $[-(MN+M-1),(MN+M-1)]$. Similarly, a k times extended coprime array is proposed to further increase the consecutive part in the difference coarray by increasing the M-elements sub-array to a (kM)-elements sub-array [25]. Another approach expands the two sub-arrays of classical coprime array from one period subarray to multi-period subarray [26] to enlarge the consecutive coarray part. In [27], the inter-element spacing of classical coprime array is designed with two integers larger than M, N such that the redundancy of coarray elements is minimized and the consecutive coarray is extended.

Filling the holes in the difference coarray is also a possible means to enlarge the difference coarray. In [28, 29], by moving the physical array at a certain velocity, the cross correlation between the received signals before and after the array motions is used to fill the holes in the difference coarray. A multiple frequency mechanism is proposed in [30] to fill all the holes such that all the DOFs provided by the difference coarray can be exploited. On the other hand, the holes can be also filled by interpolation based techniques. The interpolation of virtual array problem can be formulated as a nuclear norm minimization problem [31] or an atomic norm interpolation problem [32]. Another interpolation technique uses the Toeplitz property of the covariance matrix to complete the covariance matrix [33, 34]. However, these interpolation techniques mainly consider the problem from the aspect of the difference coarray. And the mutual coupling effect has not been considered.

Most recently, the thinned coprime array (TCA) [35] shows that some sensors in a coprime array are found to be redundant. In other words, the difference coarray structure will not be modified if these redundant sensors are removed from the coprime array. Same DOFs and less mutual coupling can be achieved with fewer sensors in TCA compared with the classical coprime array [21]. Though TCA can achieve higher DOFs compared to the classical coprime array for a given number of sensors, there are still many holes in the difference coarray. Based on the extended coprime array [25], some additional sensors are added to construct a complementary coprime array (CCA) and fill the holes in the difference coarray. However, CCA requires $(M-1)$ additional sensors to fill the holes and totally $3M+N-2$ sensors are required, which is not an economical solution when M is large. Also, the introduced sensors in CCA are closely distributed with inter-element spacing equal to half of the wavelength of incoming signals. The mutual coupling is unavoidable as the number of sensors increases.

In this paper, we focus on DOA estimation with a new coprime array configuration. This paper has two principal objectives. 1) Fill as many holes as possible to enlarge the consecutive part of the difference coarray by properly rearranging few sensors without additional new sensors. 2) Reduce the mutual coupling simultaneously. In recent research, the position of every hole has been given in [25, 36]. Without loss of generality, in this paper, we consider the mostly used generalized CA, corresponding to the CACIS configuration with $2M+N-1$ sensors (compression factor $p=2$) [24], which is also a specific case of the k-times extended coprime array with $k=2$ [25]. In the following, we call this generalized coprime array as classical or conventional coprime array. Inspired by the fact that few sensors in the conventional coprime array are redundant, we propose a rearranged coprime array for which these redundant sensors are relocated in order to fill most of the holes (even all the holes).

To the best of our knowledge, our proposed configuration is the first work to fill the holes from the view of rearranging few physical sensors in the classical coprime array without introducing additional new sensors. Only the redundant sensors in the classical coprime array are utilized such that no extra hardware cost is required. The proposed rearranged coprime array can keep the main advantages of TCA, i.e. closed-form expression of sensor position, low mutual coupling, easy to choose M, N values. The proposed configuration consists of four sparse sub-arrays where two sub-arrays form a TCA and the other two sub-arrays are relocated outside the TCA. As illustrated in the following sections, our proposed configuration can detect more sources than TCA and the conventional coprime array for a given number of sensors. Another distinguished

benefit of the proposed configuration is the reduction of mutual coupling. The performance of the proposed configuration under high mutual coupling is shown, by simulations, to be better than the compared sparse arrays.

The rest of this paper is organized as follows. Section II provides a review of the difference coarray based signal model and the conventional coprime array structure. The proposed rearranged coprime array configuration is described in Section III. The properties of the proposed configuration are highlighted in Section IV. Numerical simulation results are given in Section V and conclusions are drawn in Section VI.

2. PROBLEM FORMULATIONS

2.1. Difference Coarray Signal Model

Assume that K far field uncorrelated narrowband sources impinge on a sparse array with L sensors, where the sensors are located at $n_i d$, $1 \leq i \leq L$, with $n_1 < n_2 < ... < n_L$ and d is equal to half of the wavelength of incoming signals. The received signal vector of the sparse array can be written as:

$$\mathbf{x}(t) = \sum_{k=1}^{K} \mathbf{a}(\theta_k) s_k(t) + \mathbf{n}(t) = \mathbf{A}\mathbf{s}(t) + \mathbf{n}(t) \tag{1}$$

where $\mathbf{s}(t) = [s_1(t), s_2(t), ..., s_K(t)]^T$ is the vector of signals received at the origin of the coordinate system, $\mathbf{n}(t)$ is the zero mean additive white Gaussian noise vector with covariance matrix $\sigma^2\mathbf{I}$; $\mathbf{A} = [\mathbf{a}(\theta_1), \mathbf{a}(\theta_2), ..., \mathbf{a}(\theta_K)]$ is the array manifold matrix with θ_k the direction of the k-th source, and $\mathbf{a}(\theta_k)$ is the corresponding steering vector, given by

$$\mathbf{a}(\theta_k) = [e^{j\pi n_1 \sin(\theta_k)}, e^{j\pi n_2 \sin(\theta_k)}, ..., e^{j\pi n_L \sin(\theta_k)}]^T \tag{2}$$

Then the covariance matrix of $\mathbf{x}(t)$ can be written as

$$\mathbf{R}_\mathbf{x} = E\{\mathbf{x}(t)\mathbf{x}(t)^H\} = \mathbf{A}\mathbf{R}_\mathbf{s}\mathbf{A}^H + \sigma^2\mathbf{I} \tag{3}$$

where $\mathbf{R}_\mathbf{s} = E\{\mathbf{s}(t)\mathbf{s}^H(t)\}$ is the source covariance matrix. $\mathbf{R}_\mathbf{x}$ can be vectorized as [10]

$$\mathbf{z} = \text{vec}(\mathbf{R}_\mathbf{x}) = (\mathbf{A}^* \odot \mathbf{A})\mathbf{p} + \sigma^2\mathbf{1}_{vec} \tag{4}$$

where $\mathbf{p} = [\sigma_1^2, \sigma_2^2, ..., \sigma_K^2]^T$ with σ_k^2 the power of the k-th source and $\mathbf{1}_{vec} = \text{vec}(\mathbf{I})$; $\odot$ is the Khatri-Rao product operator. The vector $\mathbf{z}$ can be equivalently considered as K coherent sources measured by a virtual array whose sensor positions are determined by the differences between the physical sensor positions. This virtual array is named as difference coarray, which can be defined as $\mathbb{D}$. The maximum consecutive part among $\mathbb{D}$ is denoted as $\mathbb{U}$. For a sparse array geometry specified by position indices set $\mathbb{S} = \{n_1, n_2, ..., n_L\}$, its difference coarray can be expressed as

$$\mathbb{D} = \{n_i - n_k | n_i, n_k \in \mathbb{S}\} \tag{5}$$

The virtual array signal model of the consecutive part $\mathbb{U}$ can be selected from $\mathbf{z}$ and rearranged as

$$\mathbf{z}_1 = \mathbf{F}\mathbf{z} = \mathbf{A}_v\mathbf{p} + \sigma^2\mathbf{F}\mathbf{1}_{vec} \tag{6}$$

where $\mathbf{F}$ is the selection matrix [10] and $\mathbf{A}_v$ is the manifold matrix of the virtual array.

2.2. Mutual Coupling

Equation (1) does not take the mutual coupling into account. In practice, the mutual coupling of two closely located sensors could strongly affect the received signal. Considering the mutual coupling, we can rewrite (1) as

$$\mathbf{x}(t) = \mathbf{C}\mathbf{A}\mathbf{s}(t) + \mathbf{n}(t) \tag{7}$$

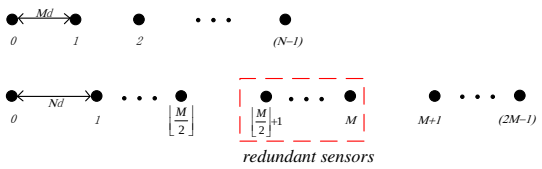

Figure 1: Conventional coprime array.

where $\mathbf{C}$ is the mutual coupling matrix. The entries of $\mathbf{C}$ can be very complicated in practice. In this paper, the considered array has a linear configuration. $\mathbf{C}$ can be approximately represented by a B-band symmetric Toeplitz matrix [18, 37] and the (i,j)-th entry of $\mathbf{C}$ is given by

$$\langle \mathbf{C} \rangle_{i,j} = \begin{cases} c_{|n_i - n_j|}, & \text{if } |n_i - n_j| \leq B \\ 0, & \text{otherwise,} \end{cases} \tag{8}$$

where $n_i, n_j \in \mathbb{S}$ and the magnitudes of coupling coefficients $c_0, c_1, ..., c_B$ meet the relations $|c_0| = 1 > |c_1| > ... > |c_B|$. The magnitudes of the coupling coefficients are assumed to be inversely proportional to their sensor separations, which can be written as

$$\frac{|c_k|}{|c_l|} = \frac{l}{k} \tag{9}$$

where l, k are positive integers indicating the separations distances between two corresponding sensors.

In the coarray, there could be several different sensor pairs that contribute to the same virtual sensor. For further discussion, the *weight function* [20] is defined as the number of sensor pairs leading to element m in the coarray

$$\mathbb{W}_m = \{(n_1, n_2) \in \mathbb{S}^2 | n_1 - n_2 = m\} \tag{10}$$

$$\omega(m) = \text{Card}(\mathbb{W}_m) \tag{11}$$

where $\omega(m)$ is the weight function and $\mathbb{W}_m$ represents the set of physical sensor pairs leading to the m-th virtual sensor in the coarray, $\text{Card}(\mathbb{W}_m)$ returns the cardinality of set $\mathbb{W}_m$.

If it is a hole at the m-th position in the coarray, $\omega(m) = 0$. It is well established that the value of the weight function corresponding to small sensor separation m has high mutual coupling effect. Particularly, the first three values $\omega(1), \omega(2), \omega(3)$ would be of great interest since they contribute primarily to the mutual coupling due to their small sensor separation [19, 20]. For simplification, we will exploit the first three values of the weight function for analytical discussion of the mutual coupling effect in the following part.

2.3. Conventional coprime array and TCA

In this subsection, we introduce some properties of the conventional coprime array and TCA. The considered array geometry consists of two sub-arrays, where one sub-array has N sensors with Md as separation distance between two adjacent sensors and another sub-array has $2M$ sensors with Nd as the distance between two adjacent sensors. The first sensor is shared by the two sub-arrays. A graphic illustration of the conventional coprime array is given in Fig. 1, where M, N are two coprime integers. In this paper, we assume $2 \leq M < N$ without loss of generality.

It is well established that there are some holes in the difference coarray of the classical coprime array. Since the difference coarray is a symmetric structure, for simple illustration, we only take the non-negative part of the difference coarray into account in the following part. The *position of holes* ranges from $MN + M$

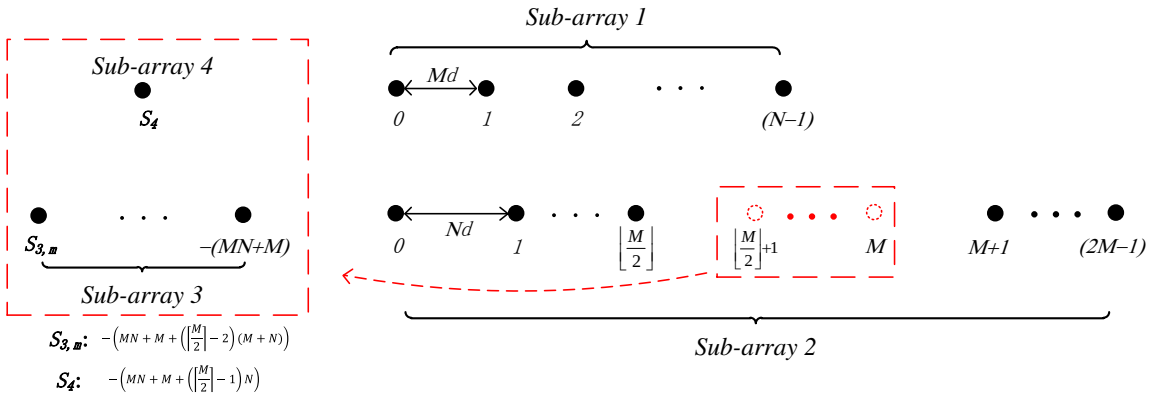

Figure 2: Position of sensors in the rearranged coprime array. • : physical sensors, ⁛ : redundant sensors of the conventional coprime array.

to $(2M-1)N$ [25, 36], and is given by

$$\begin{aligned} \mathbb{H} &= \{h | h = MN + M + b_1 M + b_2 N\}, \\ s.t. \quad 0 \le b_1 \le N - 2 - \lfloor \frac{N}{M} \rfloor, &\quad 0 \le b_2 \le M - 2, \\ h &\in [MN + M, (2M-1)N) \end{aligned} \tag{12}$$

In the conventional coprime array, it has been proved that some sensors in the $2M$-elements sub-array are redundant [21, 35]. In other words, removing these redundant sensors will not change the difference coarray geometry. As shown in Fig. 1, by removing the redundant sensors in the rectangle, the conventional coprime array turns out to be a TCA.

The number of contiguous redundant sensors for a conventional coprime array (except for $M = 3$) is given by

$$S_{red} = \lceil \frac{M}{2} \rceil \tag{13}$$

where these redundant sensors are all in the $2M$-elements sub-array and the index of these redundant sensors starts from $\lfloor \frac{M}{2} \rfloor + 1$. The symbol $\lceil x \rceil$ returns the smallest integer greater than x and $\lfloor x \rfloor$ denotes the greatest integer less than x. The proof for the redundancy of these sensors can be found in [21].

The case of $M = 3$ is special, for which, there are still $\lceil \frac{M}{2} \rceil = 2$ redundant sensors in the $2M$-elements sub-array. However, these two redundant sensors are no longer contiguous. Their positions are MNd and Nd. The redundancy of sensor at position MNd has been proved in [21]. By applying the similar derivation, we can also prove the redundancy of the sensor positioned at Nd.

3. PROPOSED REARRANGED COPRIME ARRAY

In the previous section, we have reviewed that the holes in the conventional coprime configuration locate in the range from $MN + M$ to $(2M-1)N$. To enlarge the consecutive part in the difference coarray, we propose a rearranged coprime array without introducing additional sensors in this section. Based on the expression of holes position, we move the redundant sensors to appropriate positions such that most of the holes (even all the holes) in $[MN + M, (2M-1)N)$ can be filled. The proposed rearranged coprime array has also closed-form expression for the position of sensors. Furthermore, the proposed configuration is more robust to the mutual coupling effect compared with most of the existing sparse arrays.

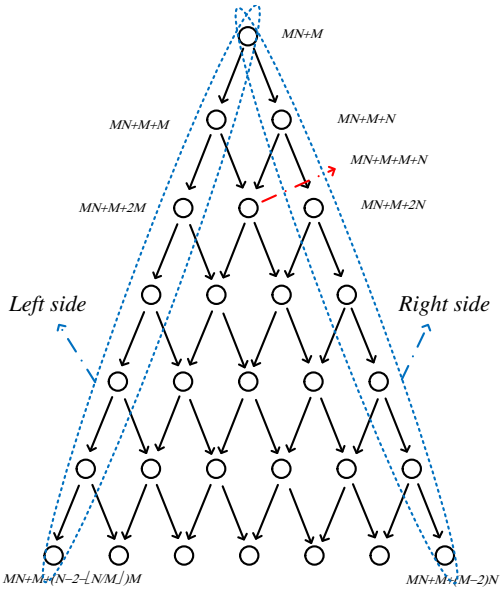

Figure 3: Holes-triangle with $M = 8, N = 9$.

3.1. Holes representation with holes-triangle

To better explain the design rules of the proposed rearranged coprime array, we first classify all the holes into a specific order with a 2D-representation. In [25], CCA method classifies the holes into several layers including $M-1$ complete layers, and $M-1$ extra sensors are required in the complementary sub-array to fill all the holes. Though CCA can fill all the holes, the way that these extra sensors are utilized to fill the holes is not efficient due to the way the holes are classified. In this section, we classify the holes into several sub-triangles, where we can fill the holes in a more efficient way. Our aim is to fill the holes only with the $\lceil \frac{M}{2} \rceil$ redundant sensors such that no extra sensor is required. We classify the holes from another point of view. Based on (12), we define holes-triangle to represent all the hole elements.

Definition 1: A *holes-triangle* is a triangle-like structure with its elements given by (12)

$$h \in \mathbb{H}. \tag{14}$$

The holes-triangle can be divided into several sub-triangles with each consisting of a *left-side* and a *right-side*. In a *sub-triangle*, starting with a given hole element h, the *left-side* is defined as the set

$$\{h + iM| \quad h + iM < (2M-1)N\} \tag{15}$$

with its elements in increasing order, and the *right-side* is defined as the set

$$\{h + kN| \quad h + kN < (2M-1)N\} \tag{16}$$

also with its elements arranged in increasing order, where i, k are two non-negative integers. The intersection element h between the *left-side* and *right-side* is called the vertex of the corresponding *sub-triangle*.

An example of holes-triangle with $M = 8, N = 9$ is given in Fig. 3. The hole elements are represented with circles and the arrows indicate the increasing direction between two neighbor elements. We emphasize the biggest sub-triangle with two dotted ovals for illustration, which has the most hole elements among all the sub-triangles. The value of elements on the left-side increases from $MN+M$ to $MN+M+(N-2-\lfloor \frac{N}{M} \rfloor)M$ while that of the right-side increases from $MN+M$ to $MN+M+(M-2)N$, as clearly indicated by (12).

3.2. Holes filling with rearranged coprime array

In [25], some additional sensors are introduced at the position corresponding to the biggest value in each left-side or right-side of some sub-triangles to fill the holes. $M-1$ additional sensors are required in the CCA method and it could be hardware expensive when M is a large value. In this paper, we aim to fill the holes without introducing extra sensors. This can be achieved by relocating the redundant sensors at specific sparse positions. By doing so, the length of $\mathbb{U}$ can be significantly increased. The position of sensors after the rearrangement can be given by:

$$\mathbb{S}_1=\{n_1M|0\leq n_1\leq N-1\} \tag{17}$$

$$\mathbb{S}_2=\{n_2N|(0\leq n_2\leq \lfloor\frac{M}{2}\rfloor)\cup(M+1\leq n_2\leq 2M-1)\} \tag{18}$$

$$\mathbb{S}_3=\{-(MN+M+i(M+N))|0\leq i\leq \lceil\frac{M}{2}\rceil-2\} \tag{19}$$

$$\mathbb{S}_4=\{-(MN+M+(\lceil\frac{M}{2}\rceil-1)N)\} \tag{20}$$

The configuration of our proposed rearranged coprime array is shown in Fig. 2. It can be observed that there are totally $(2M+N-1)$ physical sensors, exactly the same as the conventional coprime array. The sub-arrays $\mathbb{S}_1$ and $\mathbb{S}_2$ form a TCA with $(2M+N-1)-\lceil\frac{M}{2}\rceil$ sensors. The $\lceil\frac{M}{2}\rceil$ redundant sensors of the original conventional coprime array are represented by red dot circles. These redundant sensors are selected and rearranged outside the TCA to construct sub-arrays $\mathbb{S}_3$ and $\mathbb{S}_4$.

The reason of rearranging the redundant sensors at $\mathbb{S}_3$ and $\mathbb{S}_4$ is based on the following properties of the holes-triangle.

Property 1: For any given conventional coprime array, if one additional sensor is positioned at the symmetric negative position of that of a sub-triangle vertex, namely $-h$, all the holes elements at the *left-side* and *right-side* of the corresponding sub-array can be filled.

Proof. Assuming a given hole position $h\in[MN+M,(2M-1)N)$ in the holes-triangle, its corresponding *left-side* and *right-side* elements can be given as set $\{h+iM|h+iM<(2M-1)N\}$ and $\{h+kN|h+kN<(2M-1)N\}$ respectively. Sensors of the conventional coprime array are located at two sub-arrays $\{n_1M|0\leq n_1\leq N-1\}$ and $\{m_1N|0\leq m_1\leq 2M-1\}$.

If one additional sensor is introduced at position $-h$, for any hole element $h+iM$ at the corresponding *left-side*, we can always find a sensor from the N-elements sub-array of the conventional coprime array such that

$$h+iM=iM-(-h) \tag{21}$$

Then the hole element $h+iM$ can be filled. Relation (21) holds for all the hole elements at the *left-side* because $0\leq i\leq N-2-\lfloor\frac{N}{M}\rfloor$ is an element of $[0,N-1]$. Similar derivation can be applied to the corresponding *right-side*. Then *Property 1* is proved. □

Since we pick out the redundant sensors and relocate them outside the TCA, *Property 1* can be modified as follows

Lemma 1: For a rearranged coprime array, if one redundant sensor is relocated at the symmetric negative position of a sub-triangle vertex, all the holes elements on the *left-side* and the first $\lfloor\frac{M}{2}\rfloor+1$ holes at the *right-side* can be filled.

Proof. Similar to the proof of *Property 1*, the elements at the *left-side* can be filled. After picking out the redundant sensors, the indexes of the first $\lfloor\frac{M}{2}\rfloor+1$ remaining sensors in the $(2M-\lceil\frac{M}{2}\rceil)$ elements sub-array are distributed in $[0,\lfloor\frac{M}{2}\rfloor]$. For a given hole position h, the following $\lfloor\frac{M}{2}\rfloor+1$ holes at the *right-side*, which are denoted as $h+kN$, can be filled by calculating the difference

$$h+kN=kN-(-h)\quad s.t.\quad 0\leq k\leq\lfloor\frac{M}{2}\rfloor \tag{22}$$

Then *Lemma 1* is proved. □

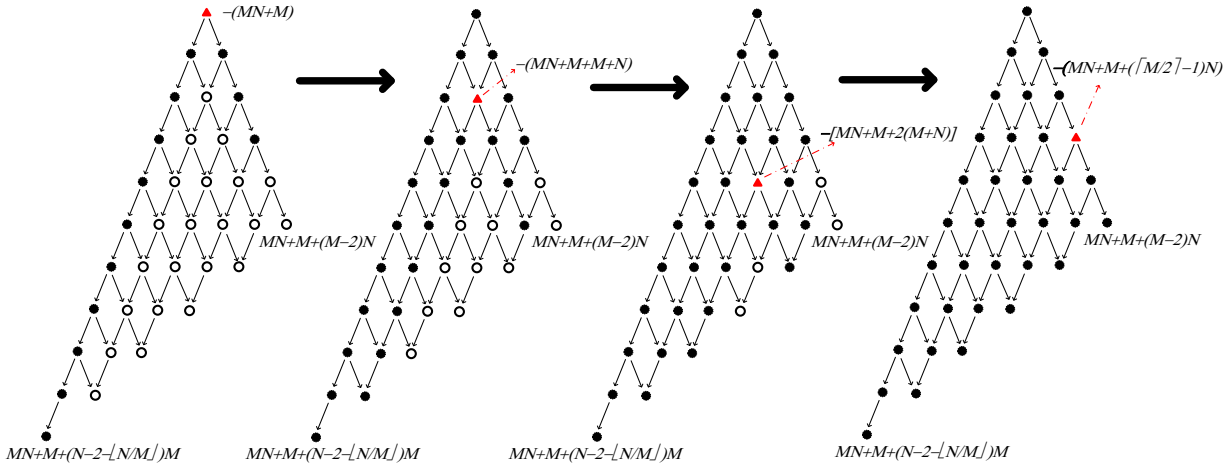

Figure 4: Holes filling with the redundant sensors. $M = 7, N = 13$ ∘ : unfilled holes; • : filled holes; ▲: rearranged sensor position.

Our goal is to fill as many holes as possible (even all holes) with the $\lceil \frac{M}{2} \rceil$ redundant sensors. For each redundant sensor, a good solution is to position it at the symmetric negative position of that of the vertex of the sub-triangle containing as much hole elements as possible. We have the following property for any two sub-triangles.

Property 2: For any two sub-triangles with vertex elements $h_1 < h_2$, the number of elements at the right-side corresponding to h_2 can not be greater than that corresponding to h_1.

Proof. This can be proved by contradiction. We assume that the elements at the right-side of h_2 are in the form $h_2 + i_2 N$. Similarly, the elements at the right-side of h_1 are $h_1 + i_1 N$. Here, $i_1 \in [0, i_{1,max}], i_2 \in [0, i_{2,max}]$. Here, we consider that h_1, h_2 are also element of their right-side. The number of right-side elements associated to h_2 greater than the number of right-side elements associated to h_1 if and only if $i_{1,max} < i_{2,max}$. On the other hand, we should have $h_2 + i_{2,max} N < (2M-1)N$. Since $h_1 < h_2$, we can easily obtain $h_1 + i_{2,max} N < (2M-1)N$, which means that the right-side of h_1 has at least $i_{2,max} + 1$ elements ($i_{1,max} \geq i_{2,max}$). This contradicts with $i_{1,max} < i_{2,max}$ and *Property 2* is proved. □

From *Property 1*, we can know that the left-sides can be easily filled. This can be achieved by rearranging $\lceil \frac{M}{2} \rceil - 1$ redundant sensors at position set $\mathbb{S}_3$. Since we have only $\lceil \frac{M}{2} \rceil$ redundant sensors to fill the holes, we particularly focus on the right-side with the largest number of elements. This will naturally lead to the solution of position $\mathbb{S}_4$. Fig. 4 is an example of the holes filling process with $M = 7, N = 13$. The highlighted red triangles indicate the position of the rearranged redundant sensors at the symmetric negative position. The hollow circles represent the unfilled holes and the solid circles are the filled holes after rearranging the redundant sensors. There are totally $\lceil \frac{M}{2} \rceil = 4$ redundant sensors in this case so we divide the holes filling process into 4 steps as shown in Fig. 4.

It can be observed from Fig. 4 that three redundant sensors are rearranged at $-[MN + M + i(M+N)]$ in the first three steps, where $0 \leq i \leq \lceil \frac{M}{2} \rceil - 2 = 2$. At the first step, according to *Lemma 1*, only the first $\lfloor \frac{M}{2} \rfloor + 1 = 4$ elements at the *right-side* can be filled with one sensor at position $-(MN + M)$. After the third step, the remaining unfilled elements, including $MN + M + (\lceil \frac{M}{2} \rceil - 1)(M+N)$, can be considered as a new sub-triangle, whose vertex is $MN + M + (\lceil \frac{M}{2} \rceil - 1)N$. Therefore, we rearrange the last redundant sensor at position $-(MN + M + (\lceil \frac{M}{2} \rceil - 1)N)$ to fill these holes.

4. Properties of the proposed rearranged coprime array

4.1. Length of contiguous difference coarray

For a given number of sensors, the cardinality of $\mathbb{U}$ will be increased if most holes are filled. Especially, we are more interested in the case where all holes in the range $[MN+M,(2M-1)N)$ can be filled. We consider the holes filling problem in two scenarios: 1) odd value of M; 2) even value of M.

Lemma 2: The rearranged coprime array has a contiguous difference coarray ranging in $[0,(2M-1)N]$ if

$$\begin{cases} N \text{ can be any integer coprime with } M, & \text{if } M=2,3 \\ 3<M\leq 7, \quad M<N<M+4+\frac{12}{M-3}, & \text{if } M \text{ is odd} \\ 2<M\leq 8, \quad M<N<M+2+\frac{4}{M-2}, & \text{if } M \text{ is even.} \end{cases} \tag{23}$$

The proof is provided in Appendix. The possible values of M,N satisfying Lemma 2 are listed in Table 1

Table 1: Possible values of M and N satisfying Lemma 2.

Possible value of M	Possible value of N
2	Odd integers greater than 2
3	Integers greater than 3 which is coprime with 3
4	5,7
5	6,7,8,9,11,12,13,14
6	7
7	8,9,10,11,12,13
8	9

It should be mentioned that even if condition (23) is not met with other values of M and N, the rearranged coprime array can still fill most of the holes in $[MN+M,(2M-1)N)$. The consecutive part of the difference coarray can still be significantly enlarged. In this case, the consecutive part ranges from 0 to h_0-1, where h_0 is the first hole in the coarray of the rearranged coprime array. Then we can derive the following Lemma.

Lemma 3: For M,N values that do not satisfy Lemma 2, the first hole occurs at

$$\begin{cases} h_0=\begin{cases} a_1, & \text{if } N<\frac{M(M-3)}{2} \\ a_2, & \text{if } N>\frac{M(M-3)}{2} \end{cases} & \text{, M is odd} \\ h_0=\begin{cases} a_1, & \text{if } N<\frac{M(M-4)}{4} \\ a_2, & \text{if } N>\frac{M(M-4)}{4} \end{cases} & \text{, M is even} \end{cases} \tag{24}$$

where $a_1=MN+2(M+N)+\lfloor\frac{M}{2}\rfloor N$ and $a_2=MN+\lceil\frac{M}{2}\rceil(M+N)$.

The proof is provided in Appendix

4.2. Weight function

Apart from a larger consecutive part in the difference coarray, another benefit of the proposed rearranged coprime array is its less mutual coupling effect. It is well known that the mutual coupling is strongly dependent on the separation distance between sensors [38, 39]. Especially, sensors with a small separation distance could experience strong mutual coupling. Since $\omega(m)$ indicates the number of physical sensor pairs contributing to separation m, we approximately quantify the mutual coupling with the help of the weight function. For simplification, we particularly focus on the first three weight function values, i.e. $\omega(1),\omega(2),\omega(3)$.

In the rearranged coprime array, sub-arrays $\mathbb{S}_1$, $\mathbb{S}_2$ form a TCA. For given values of M and N, the corresponding first three weight function values of TCA, denoted as $\omega^{'}(1),\omega^{'}(2),\omega^{'}(3)$, have been provided in [21]. Considering the contribution of sub-arrays $\mathbb{S}_3$, $\mathbb{S}_4$, we have the following property.

Property 3: For the proposed rearranged coprime array, the interaction between $\mathbb{S}_3$ and $\mathbb{S}_4$ contributes at most one additional value to either one of $\omega^{'}(1), \omega^{'}(2), \omega^{'}(3)$, which can be formulated as:

$$\omega(1)+\omega(2)+\omega(3) \leq \omega^{'}(1)+\omega^{'}(2)+\omega^{'}(3)+1 \tag{25}$$

Proof. The interaction between $\mathbb{S}_1$ and $\mathbb{S}_2$ leads to $\omega^{'}(1), \omega^{'}(2), \omega^{'}(3)$. The minimum spacing between any element in $\mathbb{S}_3$, $\mathbb{S}_4$ and any element in $\mathbb{S}_1$, $\mathbb{S}_2$ is $M+N \geq 5$. This means that the cross interaction between $\mathbb{S}_3$, $\mathbb{S}_4$ and $\mathbb{S}_1$, $\mathbb{S}_2$ has zero contribution to $\omega(1), \omega(2)$ and $\omega(3)$. Therefore, we only need to consider the interaction between $\mathbb{S}_3$ and $\mathbb{S}_4$. The minimum spacing between the elements in $\mathbb{S}_3$ equals to $M+N$ such that the self-interaction of $\mathbb{S}_3$ has zero contribution to $\omega(1), \omega(2), \omega(3)$. On the other hand, $\mathbb{S}_4$ has only one sensor. The cross interaction between $\mathbb{S}_3$ and $\mathbb{S}_4$ can be divided into two scenarios:

(1) $(\lceil \frac{M}{2} \rceil - 2)(M+N) < (\lceil \frac{M}{2} \rceil - 1)N$;

(2) $(\lceil \frac{M}{2} \rceil - 2)(M+N) > (\lceil \frac{M}{2} \rceil - 1)N$.

In the first scenario, the only possible cross-interaction contributing to $\omega(1), \omega(2), \omega(3)$ is $d_1 = (\lceil \frac{M}{2} \rceil - 1)N - (\lceil \frac{M}{2} \rceil - 2)(M+N)$. This is obvious because for other cross-interactions, they hold the form $d_1 + k(M+N)$, which is greater than 5.

In the second scenario, there are two closest sensors in $\mathbb{S}_3$ (with spacing $M+N$) located at the left and right sides of $\mathbb{S}_4$. Assuming the distances of $\mathbb{S}_4$ to the nearest two sensors in $\mathbb{S}_3$ which located at the left and right side of $\mathbb{S}_4$ are $d_1^{'}$ and $M+N-d_1^{'}$, respectively. It is obvious that $d_1^{'}$ and $M+N-d_1^{'}$ are the only two possible contributions to $\omega(1), \omega(2), \omega(3)$. Due to the coprime property of M, N, the minimum value of $M+N$ is 5 for $M=2, N=3$. With $M=2, N=3$, there is only one redundant sensor located at $\mathbb{S}_3$ and it brings no contribution to $\omega(1), \omega(2), \omega(3)$. For other values of M, N, $M+N \geq 7$ and the following conditions can not hold simultaneously.

$$d_1^{'} \leq 3 \tag{26}$$

$$M+N-d_1^{'} \leq 3 \tag{27}$$

This means that $d_1^{'}$ and $M+N-d_1^{'}$ contribute at most one value to either one of $\omega(1), \omega(2), \omega(3)$. *Property 3* is then proved. □

For information purpose, let's derive the special case when $\omega(1)=2$.

Since $\omega(1)$ contributes the most to the mutual coupling, we especially investigate $\omega(1)$ for different values of M. It has been proved that $\omega'(1)=2$ only when $M=2$ for TCA. From the above discussion, it is obvious that our method will not increase $\omega(1)$ when $M=2$. This is because there is only one redundant sensor and the rearrangement of this redundant sensor will not change $\omega(1)$, which means $\omega(1)=\omega'(1)=2$ for $M=2$.

When $M>2$, we assume the case that the interaction between $\mathbb{S}_3$ and $\mathbb{S}_4$ contributes one value to $\omega(1)$, which can be formulated as

$$-(MN+M+i(M+N)) = -(MN+M+(\lceil \frac{M}{2} \rceil - 1)N) \pm 1 \tag{28}$$

where $0 \leq i \leq \lceil \frac{M}{2} \rceil - 2$. Then we can obtain

$$N = \frac{iM \pm 1}{\lceil \frac{M}{2} \rceil - 1 - i} \tag{29}$$

Only when the value of N meets condition (29), the relation $\omega(1)=\omega'(1)+1=2$ is satisfied. Notice that $N>M$ and $M>2$ as assumed above, only a few values of N will have contribution to $\omega(1)$ for a given value of M. For example, with $M=6$, only $N=7$ meets condition (29). For other cases, our method holds a low value of $\omega(1)=1$, which allows us to attenuate the mutual coupling.

Compared with other sparse array configurations, it has been proved that though second order super nested array has small values of $\omega(1), \omega(3)$, the value of $\omega(2)$ could increase with the array size. Similar phenomenon could also happen to ANA1, ANA2 and MRA [21]. TCA can obtain low values for $\omega(1), \omega(2), \omega(3)$. The proposed rearranged coprime array has similar $\omega(1), \omega(2), \omega(3)$ property with TCA. Making the proposed rearranged coprime array structure a promising strategy to decrease the mutual coupling effect.

4.3. Holes filling ratio

Furthermore, since the number of redundant sensors is limited to $\lceil \frac{M}{2} \rceil$, it is important to fill the holes in an efficient way. We define the *holes filling ratio* to evaluate the holes filling efficiency.

Definition 2: For a given number of sensors that are relocated to fill the holes, the holes filling ratio is defined as the number of holes that can be filled by these sensors

$$r = \frac{\text{Card}(\mathbb{H}) - \text{Card}(\mathbb{H}^{'})}{S_r} \tag{30}$$

where, $\text{Card}(\mathbb{H})$ and $\text{Card}(\mathbb{H}^{'})$ are the cardinalities of hole elements between $[MN+M, (2M-1)N)$ before holes filling and after holes filling respectively. S_r is the number of rearranged sensors, i.e. $S_r = \lceil \frac{M}{2} \rceil$ for the proposed rearranged coprime array and $S_r = M-1$ for CCA since it requires $M-1$ additional sensors to fill the holes. We consider our proposed method and CCA here because they both aims to fill holes with a given number of sensors. A higher value of r indicates that the rearranged sensors can fill more holes.

It can be derived that for given values of M and N, if the CCA mechanism and rearranged coprime array can fill the same number of the holes, the proposed rearranged coprime array could achieve higher value of r because $\lceil \frac{M}{2} \rceil \leq M-1$. With bigger value of M, the difference between $\lceil \frac{M}{2} \rceil$ and $M-1$ becomes larger and the proposed array can achieve a higher r. Even in the case that the rearranged coprime array cannot fill all the holes but fill most holes, it could still achieve a high value of r.

4.4. DOFs comparison with other coprime based configurations

To fairly compare our proposed method with the other coprime based methods, we consider the optimum values of coprime integers M, N for different methods for a given number of sensors. In the following, we denote M, N for the conventional coprime array and our proposed method, M_c, N_c for CCA and M_t, N_t for TCA. It is obvious that our proposed method can achieve larger consecutive coarray than the conventional coprime array because it fills the holes in the coarray constructed from the conventional coprime array.

For comparison with TCA and CCA, we consider the case where our method can not fill all the holes. In this case, we denote the consecutive coarray length by $\min(a_1, a_2)$, with $a_1 = MN + 2(M+N) + \lfloor \frac{M}{2} \rfloor N$ and $a_2 = MN + \lceil \frac{M}{2} \rceil (M+N)$.

By referring to the selection strategy of CCA [25], M_c, N_c rely on the maximum number of DOFs and can not be directly compared with our proposed method. We compare our method and CCA from another point of view. Given $L = 2M + N - 1$ sensors, without loss of generality, we assume that $a_1 < a_2$ for our method such that the consecutive coarray length is a_1. Then we calculate M_c, N_c for CCA by assuming that its maximum number of DOFs is a_1. From [25] it comes that CCA requires $3M_c + N_c - 2$ sensors. If $3M_c + N_c - 2 > L$, then CCA requires more than L sensors to achieve the maximum number of DOFs of a_1. In the Appendix part "DOFs comparison with CCA", we have proved that $3M_c + N_c - 2 - L > 0$ for a given value of L, which indicates the superiority of the proposed method compared to CCA.

To compare with TCA, we notice that there are $\lceil \frac{M_t}{2} \rceil$ sensors which can be removed. If $M_t = M, N_t = N$, TCA has less sensors than the conventional coprime array. In other words, for a given total number of sensors $L = 2M + N - 1$, M_t, N_t should be selected as two values bigger than M, N to construct a TCA with L sensors. Without loss of generality, we assume that $M_t = M + y_1$, $N_t = N + y_2$ with $y_1, y_2 \geq 0$ and the total number of sensors in TCA is $L = 2M + N - 1$. It is obvious that $2y_1 + y_2 = \lceil \frac{M_t}{2} \rceil$ and the consecutive coarray length of TCA is $M_t N_t + M_t$.

For the choice of parameters M_t, N_t, the values of M_t, N_t can be determined similarly to M, N of the conventional coprime array since TCA is developed from conventional coprime array. The optimum values of M, N meet the condition $N = 2M - 1 = \frac{L}{2}$ when L is an even value [24]. Similarly, we assume that $2M_t + N_t - 1$ is also an even value (greater than L) and the optimum values of M_t, N_t are determined by condition $N_t = 2M_t - 1$. Then we can derive that the proposed method has larger DOFs compared to TCA for a given value of L. The proof is given in the Appendix part "DOFs comparison with TCA".

A graphic comparison of DOFs with different geometries is provided in Figure 5. In Figure 5, we consider the cases where our proposed method satisfies condition (23) and does not satisfy condition (23) (in region

$L > 20$). It can be observed that the proposed method performs better than the compared methods. Based on the above discussion, our method can achieve larger consecutive coarray part than the existing coprime based configurations.

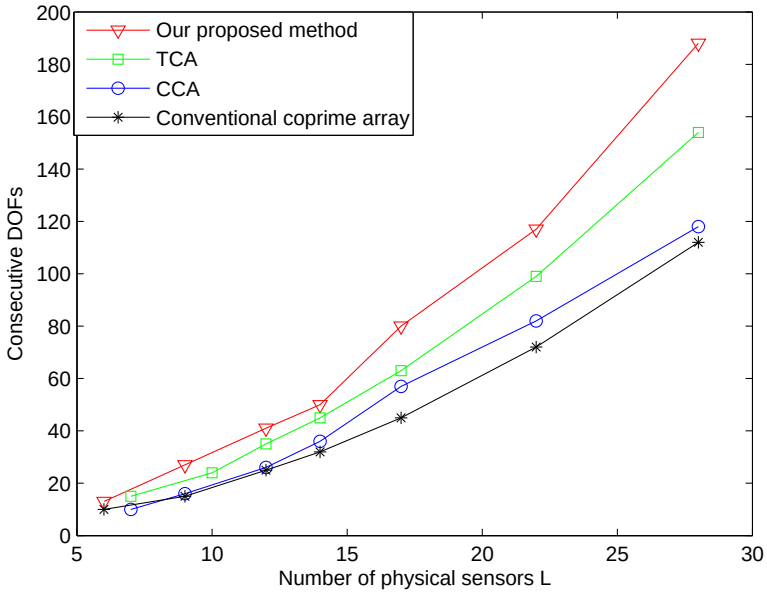

Figure 5: DOFs comparison with different coprime based configurations.

5. NUMERICAL EXAMPLES

In this section, we evaluate the holes filling ratio and the weight function for several sparse arrays. The DOA performance is assessed by applying the spatial smoothing based (SS) MUSIC algorithm. Several sparse arrays are considered for comparison, including the nested array, second order SNA (Q=2), third order SNA (Q=3), MRA, ANA1, ANA2, CCA, TCA. Since the conventional coprime array has the same difference coarray as TCA for the same values of M and N, we only take TCA for comparison.

5.1. Holes filling ratio

We first examine the holes filling ratio. The method we used for comparison is CCA. It should be mentioned that the CCA method utilizes additional sensors to fill the holes while our rearranged coprime array uses only the redundant sensors from the original conventional coprime array. From this point of view, our method is more hardware economic compared to CCA. To assure that M and N are coprime, we set $N = M + 1$. It can be seen from Fig. 6 that when M is small, the holes filling ratio of CCA and the proposed rearranged coprime array is very close. As M becomes larger, the proposed rearranged coprime array surpasses CCA and the difference between the two methods becomes larger, which indicates that each rearranged sensor of our proposed method can fill more holes than that of CCA.

5.2. Weight function

Then we compare the weight function of the nested array, ANA2, MRA, SNA (Q=2), TCA, CCA with the proposed configuration. 14 sensors are considered in this part. For the proposed array, we set $M = 4, N = 7$. The sensor positions of MRA are given in the set $\{0, 1, 2, 8, 15, 16, 26, 36, 46, 56, 59, 63, 65, 68\}$ [20]. For CCA, we set $M = 3, N = 7$. It can be observed from Fig. 7 that the nested array and CCA have high values of

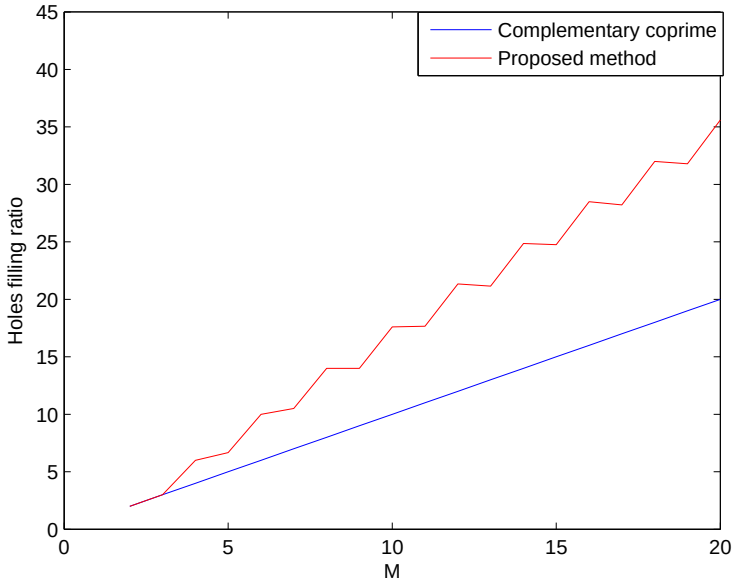

Figure 6: Holes filling ratio curves for the proposed method and CCA, $N = M + 1$.

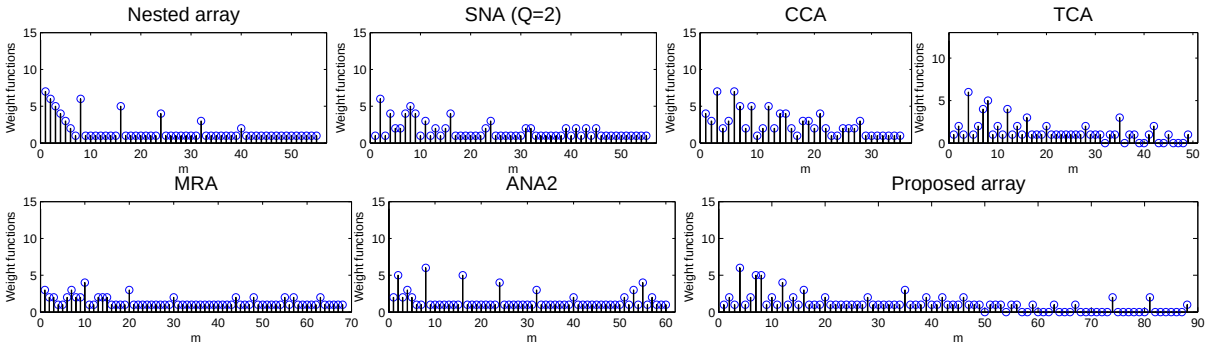

Figure 7: Weight function of seven different arrays.

$\omega(1), \omega(2), \omega(3)$, which are $\omega(1) = 7, \omega(2) = 6, \omega(3) = 5$ for the nested array and $\omega(1) = 4, \omega(2) = 3, \omega(3) = 7$ for CCA. The ANA2 and SNA (Q=2) have small values of $\omega(1), \omega(3)$ but still hold a high value of $\omega(2)$, which are $\omega(2) = 5$ and $\omega(2) = 6$ respectively. The MRA achieves $\omega(1) = 3$ and $\omega(2) = \omega(3) = 2$ while TCA has smaller value of $\omega(1) = 1$, $\omega(2) = 2$ and $\omega(3) = 1$. Though CCA can fill all the holes, the length of the difference coarray is limited to 35, which is only slightly larger than the consecutive part of TCA (31 as shown in Fig. 7). This is due to the small value of M. The proposed method achieves the same $\omega(1), \omega(2), \omega(3)$ as TCA. It can also be noticed that TCA has some holes which are denoted as set $\{32, 36, 39, 40, 43, 44, 46, 47, 48\}$, while the proposed array can fill all these elements.

An interesting fact is that the proposed strategy can also lead to some additional DOFs beyond $(2M - 1)N$, which are the elements greater than 49 in Fig. 7. These additional DOFs can be used if the compressive sensing based DOA estimation methods are applied [40, 41]. By doing so, the proposed method can detect even more sources. In this paper, our main concern is to fill the holes and enlarge the consecutive part. We only consider the SS-MUSIC afterward.

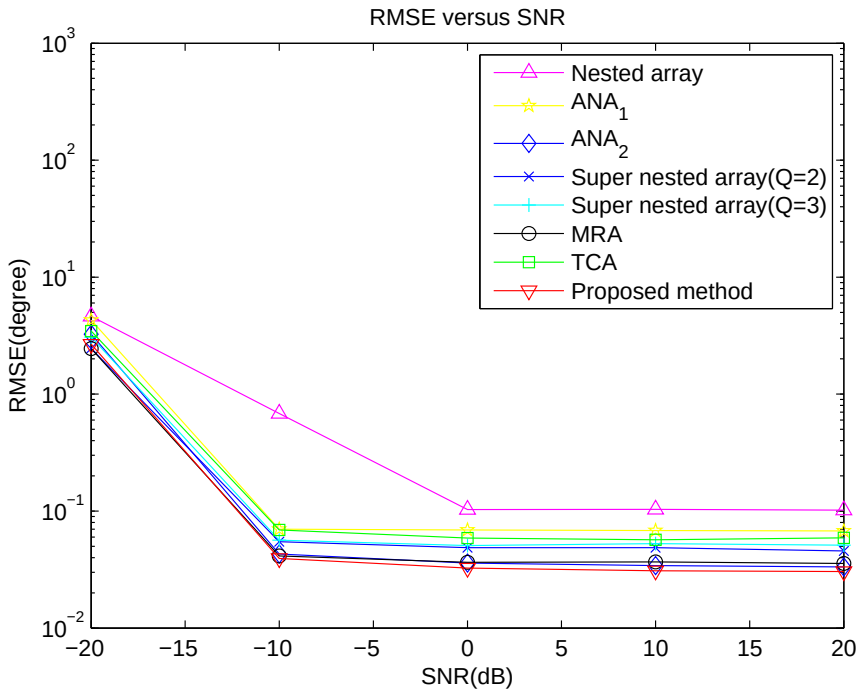

Figure 8: RMSE versus input SNR with 18 sensors, 12 sources, 1000 snapshots, $|c_1| = 0.3$.

5.3. RMSE

Next, we take the mutual coupling effect into account and evaluate the root mean square error (RMSE) of these sparse arrays. The commonly adopted SS-MUSIC is used for DOA estimation and the number of impinging signals is assumed to be known. As illustrated above, though CCA can fill the holes, the length of its difference coarray is dramatically limited and it also has a high value of $\omega(1), \omega(2), \omega(3)$. For a fair comparison, we will not compare CCA in this part. The RMSE of DOA estimation is calculated by

$$RMSE = \sqrt{\frac{1}{500K}\sum_{i=1}^{500}\sum_{k=1}^{K}(\hat{\theta}_{ki} - \theta_k)^2} \tag{31}$$

where $\hat{\theta}_{ki}$ is the estimate of θ_k in the i-th estimation trial.

The number of sensors is set to 18 and $M = 5, N = 9$ are considered for the proposed rearranged coprime array. Notice that TCA only requires 15 sensors in this case and 3 redundant sensors are not used. For a fair comparison, we set $M = 7,\ N = 9$ for TCA such that a totally of 18 sensors can be utilized. By setting a larger M value, the consecutive part of TCA is increased and the respective inter-element spacing is also increased. The sensor positions of MRA are given by the set $\{0, 1, 8, 18, 28, 38, 48, 58, 68, 78, 88, 90, 92, 94, 97, 99, 101, 103\}$ [11].

Fig. 8 and Fig. 9 examine the performance versus SNR. The number of snapshots is set to 1000 and the mutual coupling parameters are set to $c_1 = |c_1|e^{j\pi/3}$ with $|c_1| = 0.3$, $c_l = c_1 e^{-j(l-1)\pi/8}/l$ and $B = 100$. When 12 sources uniformly located between $-40°$ and $40°$ impinge on the sparse arrays, the nested array exhibits the worst performance due to its closely distributed sensors. Our proposed method achieves the best performance compared to other methods as shown in Fig. 8. In the case with more sources than sensors (25 sources in Fig. 9), ANA1 and ANA2 have worse performance than SNA since they still have higher value of $\omega(1)$, $\omega(3)$ as shown in Table 2. The proposed method can show very similar performance as MRA, which is slightly better than the first few orders of SNA (Q=2, Q=3).

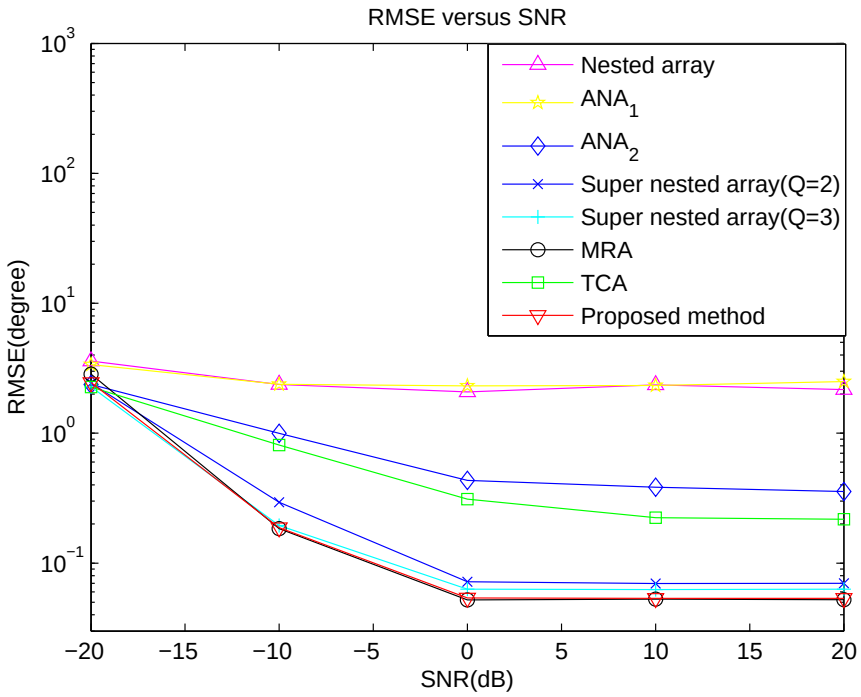

Figure 9: RMSE versus input SNR with 18 sensors, 25 sources, 1000 snapshots, $|c_1| = 0.3$.

Table 2: Weight function and maximum detectable sources with 18 sensors.

	$\omega(1)$	$\omega(2)$	$\omega(3)$	max sources
Nested array	9	8	7	89
ANA2	2	7	2	96
MRA	1	6	1	103
SNA(Q=2)	1	8	1	89
TCA	1	1	1	69
Proposed array	1	1	1	86

For a clear comparison, we also give the weight function and the maximum number of detectable sources (max sources) with 18 sensors for SS-MUSIC in Table 2. The proposed method and TCA show the lowest value of $\omega(1), \omega(2), \omega(3)$. An interesting phenomenon can also be observed that the proposed method can detect up to 86 sources in this case, which is greater than $(2M-1)N = 81$ and very close to that of SNA. This means that when the proposed strategy rearranges the redundant sensors to fill the holes within $[MN+M, (2M-1)N)$, they may also further enlarge the consecutive part to a value greater than $(2M-1)N$ simultaneously. This phenomenon happens for several different values of M, N. On the other hand, the TCA can only detect 69 sources even though higher values of $M = 7, N = 9$ are used in this case.

Fig. 10 and Fig. 11 compare the performance in terms of different number of snapshots. SNR is set to 0dB and $|c_1| = 0.3$ is used. As the increase of the number of snapshots, the performance tends to different stable values for all methods. The length of TCA consecutive part limits its performance, while the proposed method can expand the consecutive part and achieve similar performance as the other arrays.

Finally, we investigate the performance under different magnitudes of mutual coupling coefficient $|c_1|$. 1000 snapshots are used and SNR is equal to 0dB. We examine the cases with fewer sources to test the high mutual coupling scenarios, 10 sources in Fig. 12 and 20 sources in Fig. 13 respectively. The performance decreases for all methods when the coupling coefficient becomes stronger. It can be observed from Fig.

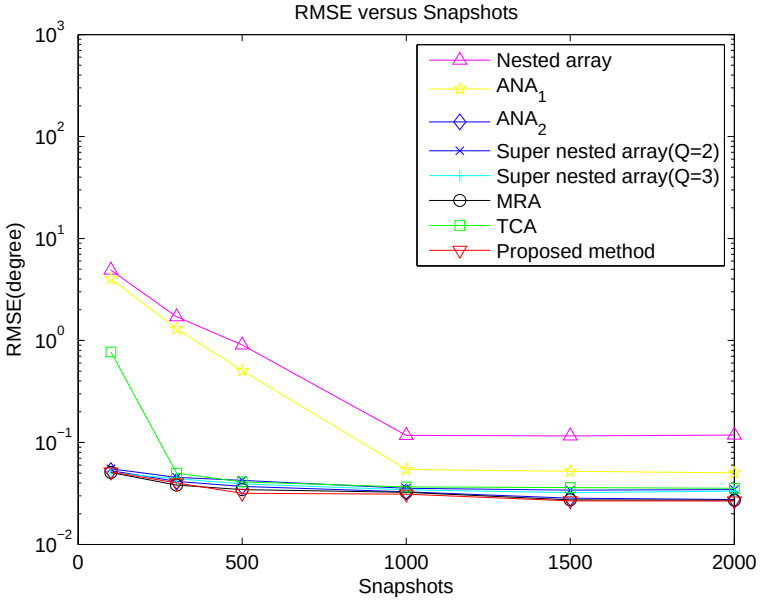

Figure 10: RMSE versus snapshots with 18 sensors, 12 sources, SNR=0dB, $|c_1| = 0.3$.

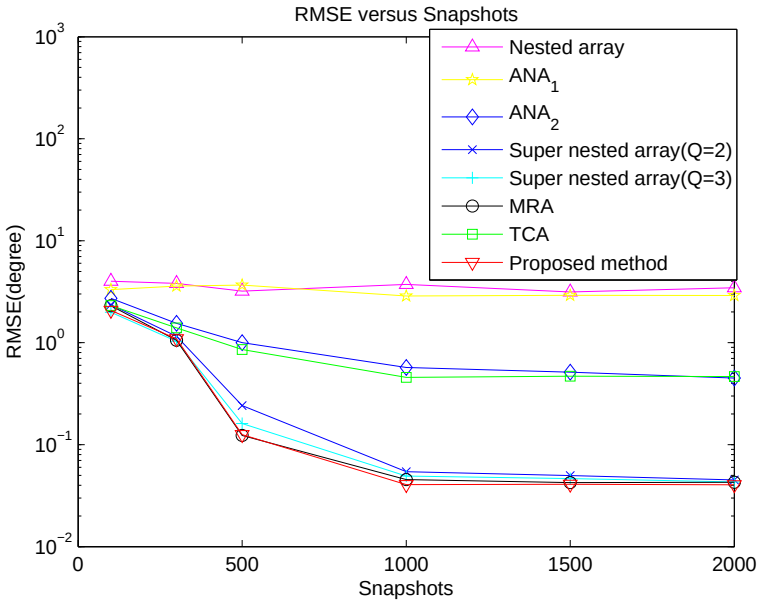

Figure 11: RMSE versus snapshots with 18 sensors, 25 sources, SNR=0dB, $|c_1| = 0.3$.

12 that the proposed array shows superiority to the other methods under high mutual coupling. Though the TCA method has small value of $\omega(1), \omega(2), \omega(3)$, its performance is affected by the short consecutive coarray. For the case of more sources than sensors, the proposed array does not exhibit significant superiority compared to other arrays in low mutual coupling region. As the coupling coefficient increases to values greater than 0.4, the proposed method starts to achieve better performance than others.

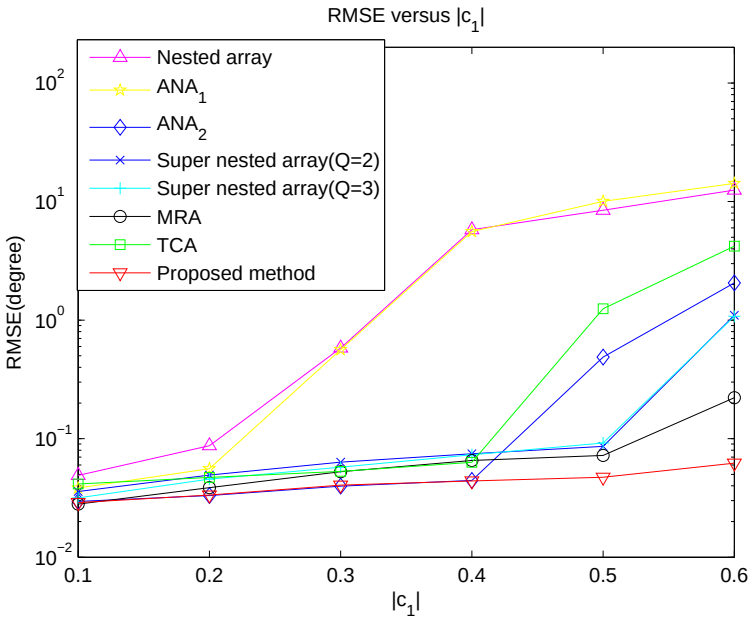

Figure 12: RMSE versus $|c_1|$ with 18 sensors, 10 sources, SNR=0dB, 1000 snapshots.

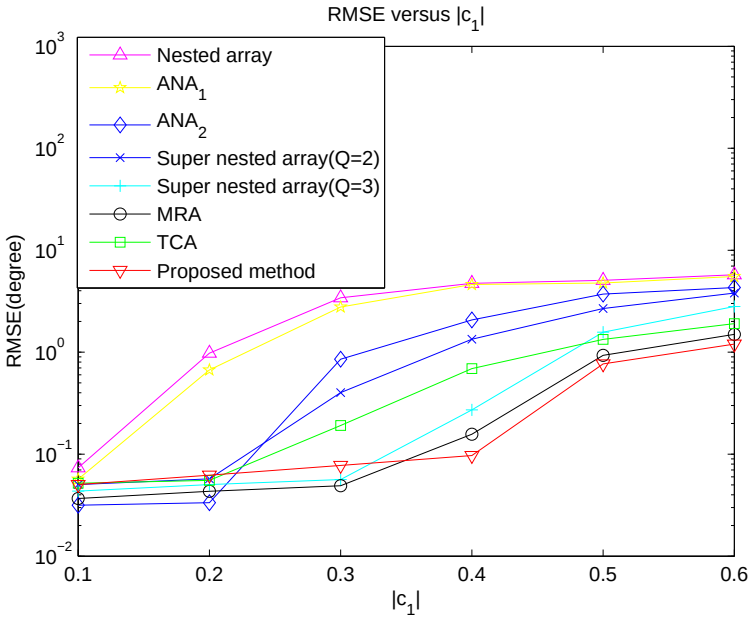

Figure 13: RMSE versus $|c_1|$ with 18 sensors, 20 sources, SNR=0dB, 1000 snapshots.

6. Conclusion

In this paper, a rearranged coprime array is proposed to fill the holes in the difference coarray of a generalized coprime array. For a given number of sensors, the proposed array can achieve larger consecutive difference coarray compared with the existing coprime based configurations, i.e. conventional coprime array, TCA, CCA. Closed-form expression of sensor positions can be calculated for the proposed method. Moreover, compared to other sparse arrays, the proposed method exhibits good performance under high mutual coupling circumstance while it can also attain comparable length of consecutive difference coarray without any additional sensor.

Acknowledgment

This work was supported in part by 2017-2019 Sino-French CAI Yuanpei Program, Guangzhou Science & Technology Program (No. 201807010071), NSFC (No. 61673260) and the China Scholarship Council (No. 201706150085).

7. Appendix

7.1. Proof of Lemma 2

From the definition of holes-triangle and *Lemma 1*, we can easily derive that the elements on the sub-triangle with vertex $MN+M$ can all be filled by arranging two sensors at positions $-(MN+M)$ and $-(MN+M+(\lceil\frac{M}{2}\rceil-1)N)$. Notice that we also have other rearranged sensors in $\mathbb{S}_3$, the left-sides corresponding to the elements of $\mathbb{S}_3$ can be filled. Assuming that there are some holes remaining unfilled, we specifically focus on the first unfilled hole with the smallest value, which is smaller than $(2M-1)N$. The position of the first unfilled hole can be divided into two scenarios.

1) If the first unfilled hole is at the sub-triangles corresponding to $\mathbb{S}_3$, this first unfilled hole will be at the right-side of the sub-triangle with vertex $MN+M+M+N$. This can be derived according to *Lemma 1* and *property 2*. Since the first $\lfloor\frac{M}{2}\rfloor+1$ elements on the right-side of vertex $MN+M+M+N$ are filled, the position of the first unfilled hole satisfies $MN+M+M+N+(\lfloor\frac{M}{2}\rfloor+1)N<(2M-1)N$. Equivalently, to assure that all holes are filled, we can formulate that

$$MN+M+M+N+(\lfloor\frac{M}{2}\rfloor+1)N>(2M-1)N \tag{32}$$

2) If the first unfilled hole is not at the sub-triangles corresponding to $\mathbb{S}_3$, we represent the unfilled holes with hollow circles in Figure 14. If we ignore the filled holes related to $\mathbb{S}_3$ for simplification, the remaining smallest element on the holes-triangle will be $MN+M+(\lceil\frac{M}{2}\rceil-1)(M+N)$ (highlighted in Figure 14). For the sub-triangle with vertex $MN+M+(\lceil\frac{M}{2}\rceil-1)(M+N)$, its left-side elements (red triangle in Figure 14) are filled by the rearranged sensor at $\mathbb{S}_4$, which is $-(MN+M+(\lceil\frac{M}{2}\rceil-1)N)$. However, the elements at the right-side of sub-triangle with vertex $MN+M+(\lceil\frac{M}{2}\rceil-1)(M+N)$ remain unfilled. In other words, the unfilled first hole will be at the right-side of the sub-triangle with vertex $MN+M+(\lceil\frac{M}{2}\rceil-1)(M+N)$. And the position of the unfilled first hole is equal to $MN+M+(\lceil\frac{M}{2}\rceil-1)(M+N)+N$. Similarly, to assure that all holes are filled, we should have

$$MN+M+(\lceil\frac{M}{2}\rceil-1)(M+N)+N>(2M-1)N \tag{33}$$

Relations (32), (33) and condition $N>M$ should both hold such that all the elements on the holes-triangle can be filled. Considering the case with M an odd integer, we can reformulate (32) as

$$MN+M+M+N+(\frac{M-1}{2}+1)N>(2M-1)N \tag{34}$$

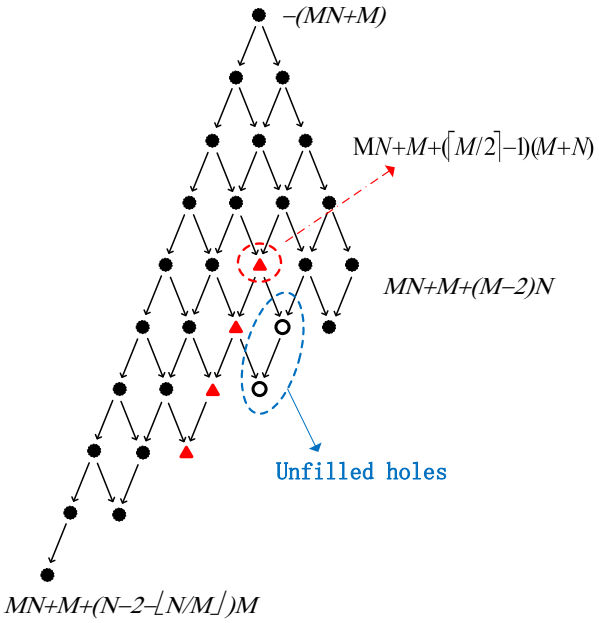

Figure 14: Position of unfilled holes with $M = 6, N = 13$. ∘ : unfilled holes; ▲: filled holes corresponding to $\mathbb{S}_4$ • : filled holes corresponding to $\mathbb{S}_3$.

After simplification, we can obtain

$$N(M-5) < 4M \tag{35}$$

Similarly, reformulating and simplifying (33), we can have

$$N < M + 4 + \frac{12}{M-3} \tag{36}$$

Notice that if $M \geq 9$, possible values of N satisfying (35) and (36) will contradict with condition $N > M$. In the case of $3 < M \leq 7$, possible values of N meeting $M < N < M + 4 + \frac{12}{M-3}$ can also satisfy (35). Following the same spirit, we can derive the expression for even value of M case, which is $M < N < M + 2 + \frac{4}{M-2}$ for $2 < M \leq 8$.

For the *special case* with $M = 3$, the two redundant sensors are not contiguous, which are located at MN and N. According to the definition of the holes-triangle, there are at most two elements at the right-side of each sub-triangle because $b_2 \leq M - 2 = 1$. Therefore, all the holes will be filled by rearranging these two redundant sensors at $-(MN + M)$ and $-(MN + M + N)$. As for the case with $M = 2$, the holes-triangle only has one left-side and they can be easily filled with one rearranged redundant sensor.

Then *Lemma 2* is proved.

7.2. Proof of Lemma *3*

If the condition in Lemma 2 is not met, there will be some unfilled holes in range $(0, (2M-1)N)$. Following the discussion in the proof of Lemma 2, considering multiple unfilled holes, the position of the first hole can be divided into two scenarios as elaborated in the proof of Lemma 2. For simplification, we reformulate the left part of the inequality in (32) and (33) as a_1, a_2 respectively, which are

$$a_1 < (2M-1)N \tag{37}$$

$$a_2 < (2M-1)N. \tag{38}$$

Either (37) or (38) holds if there are holes unfilled. If M is an odd value, without loss of generality, it can be assumed that the unfilled first hole occurs at position a_1, which means

$$a_1 < a_2. \tag{39}$$

Then it comes that $N < \frac{M(M-3)}{2}$ for (39). Similarly, if we assume $a_1 > a_2$, the result will be $N > \frac{M(M-3)}{2}$.

In the case where M is an even value, we can follow a similar derivation. Notice that a_1, a_2 differ from the case of odd value M because a_1 includes floor operator and a_2 includes ceil operator. Then if we assume $a_1 < a_2$, the result will be $N < \frac{M(M-4)}{4}$. Lemma 3 is then proved.

7.3. DOFs comparison of proposed method and CCA

We first consider L as an even value. In this case, the choice of optimal values of M, N has been proved in [24]. We follow the same principal in [24] to set the two coprime integers of our method, which are $M = \frac{L+2}{4}, N = \frac{L}{2}$. Substituting these M, N values to a_1 and simplifying, we obtain

$$a_1 > a_1' = \frac{3L^2 + 22L + 16}{16} \tag{40}$$

Then we assume that a_1' is the maximum number of DOFs of CCA, the values of M_c, N_c can be given as [25]

$$M_c = \sqrt{\frac{a_1'}{6}} + \frac{1}{2} \tag{41}$$

$$N_c = \sqrt{\frac{3a_1'}{2}} \tag{42}$$

Therefore

$$\begin{aligned} 3M_c + N_c - 2 - L &= \sqrt{6a_1'} - (\frac{1}{2} + L) \\ &= \sqrt{\frac{9L^2 + 66L + 48}{8}} - \sqrt{\frac{8L^2 + 8L + 2}{8}} \end{aligned} \tag{43}$$

Given that $L > 0$, it is obvious that the difference in (43) is greater than 0, meaning that more sensors are required by CCA to obtain a given number of DOFs compared with our method. Similarly, when we assume $a_2 < a_1$, we can obtain the same conclusion by similar derivation.

For an odd value of L, the two coprime integers of our method are $M = \frac{L+1}{4}, N = \frac{L+1}{2}$. Similarly, substituting M, N to a_1, we can still have the inequality $a_1 > a_1'$ and implement the same derivation as the even value case. Then we can get the conclusion that our method can achieve larger consecutive coarray part than CCA with a given number of sensors.

7.4. DOFs comparison of proposed method and TCA

The optimum values of N_t, M_t meet the condition $N_t = 2M_t - 1$, similarly, we have $N = 2M - 1$. Notice that $M_t = M + y_1, N_t = N + y_2$, we can derive that

$$y_2 = 2y_1 \tag{44}$$

Also notice that $2y_1 + y_2 = \lceil \frac{M_t}{2} \rceil$, which leads to

$$y_1 = \frac{1}{4} \lceil \frac{M_t}{2} \rceil \tag{45}$$

Then it can be derived that

$$\begin{aligned} M_t &= M + y_1 = M + \frac{1}{4}\lceil\frac{M_t}{2}\rceil \\ &< M + \frac{1}{4}(\frac{M_t}{2} + 1) \end{aligned} \tag{46}$$

Reformulating (46), the following inequality can be obtained

$$-(M_t N_t + M_t) = -2M_t^2 > -\frac{8}{49}(4M+1)^2 \tag{47}$$

Therefore

$$\begin{aligned} a_1 - (M_t N_t + M_t) &= a_1 - 2M_t^2 \\ &> 3M^2 + \frac{5M}{2} - 1 - 2M_t^2 \end{aligned} \tag{48}$$

Substituting (47), it can be easily shown that $a_1 - (M_t N_t + M_t) > 0$. Similarly, we can also get $a_2 - (M_t N_t + M_t) > 0$, which indicates that our method can achieve a larger consecutive coarray part than TCA.

If L is an odd value, the optimum values of $M = \frac{L+1}{4}, N = \frac{L+1}{2}$ satisfy $N = 2M$. We can also assume that $2M_t + N_t - 1$ is an odd value such that the optimum $N_t = 2M_t$. Similarly, $y_2 = 2y_1$ also holds for this case and (47) can be written as

$$-(M_t N_t + M_t) = -(2M_t^2 + M_t) > -\frac{8}{49}(4M+1)^2 - \frac{2}{7}(4M+1) \tag{49}$$

We can derive that $a_1 - (M_t N_t + M_t) > 0$ also holds for this case. Furthermore, the same conclusion can be achieved if $2M_t + N_t - 1$ is an even value. Our proposed method is shown to have larger consecutive DOFs than TCA.

[1] M. G. Amin, X. Wang, Y. D. Zhang, F. Ahmad, E. Aboutanios, Sparse arrays and sampling for interference mitigation and DOA estimation in GNSS, Proceedings of the IEEE 104 (6) (2016) 1302–1317 (June 2016). doi:10.1109/JPROC.2016.2531582.

[2] S. Haykin, Array signal processing, Englewood Cliffs, NJ, Prentice-Hall, Inc., 1985, 493 p. For individual items see A85-43961 to A85-43963. (1985).

[3] S. Chandran, Advances in direction-of-arrival estimation, Artech House Norwood, Mass, USA, 2006 (2006).

[4] J. Li, Y. Wang, C. Le Bastard, Z. Wu, S. Men, Low-complexity high-order propagator method for near-field source localization, Sensors 19 (1) (2019) 54 (2019).

[5] Q. Shen, W. Liu, W. Cui, S. Wu, Underdetermined DOA estimation under the compressive sensing framework: A review, IEEE Access 4 (2016) 8865–8878 (2016). doi:10.1109/ACCESS.2016.2628869.

[6] C. Liu, P. P. Vaidyanathan, Maximally economic sparse arrays and cantor arrays, in: 2017 IEEE 7th International Workshop on Computational Advances in Multi-Sensor Adaptive Processing (CAMSAP), 2017, pp. 1–5 (Dec 2017). doi:10.1109/CAMSAP.2017.8313139.

[7] A. Moffet, Minimum-redundancy linear arrays, IEEE Transactions on Antennas and Propagation 16 (2) (1968) 172–175 (March 1968). doi:10.1109/TAP.1968.1139138.

[8] P. Pal, P. P. Vaidyanathan, Nested arrays: A novel approach to array processing with enhanced degrees of freedom, IEEE Transactions on Signal Processing 58 (8) (2010) 4167–4181 (Aug 2010). doi:10.1109/TSP.2010.2049264.

[9] R. T. Hoctor, S. A. Kassam, The unifying role of the coarray in aperture synthesis for coherent and incoherent imaging, Proceedings of the IEEE 78 (4) (1990) 735–752 (April 1990). doi:10.1109/5.54811.

[10] M. Wang, A. Nehorai, Coarrays, MUSIC, and the Cramér-Rao bound, IEEE Transactions on Signal Processing 65 (4) (2017) 933–946 (Feb 2017). doi:10.1109/TSP.2016.2626255.

[11] M. Ishiguro, Minimum redundancy linear arrays for a large number of antennas, Radio Science 15 (06) (1980) 1163–1170 (Nov 1980). doi:10.1029/RS015i006p01163.

[12] E. Vertatschitsch, S. Haykin, Nonredundant arrays, Proceedings of the IEEE 74 (1) (1986) 217–217 (Jan 1986). doi:10.1109/PROC.1986.13435.

[13] P. P. Vaidyanathan, P. Pal, Sparse sensing with co-prime samplers and arrays, IEEE Transactions on Signal Processing 59 (2) (2011) 573–586 (Feb 2011). doi:10.1109/TSP.2010.2089682.

[14] S. Qin, Y. D. Zhang, M. G. Amin, A. M. Zoubir, Generalized coprime sampling of Toeplitz matrices for spectrum estimation, IEEE Transactions on Signal Processing 65 (1) (2017) 81–94 (Jan 2017). doi:10.1109/TSP.2016.2614799.

[15] Z. Shi, C. Zhou, Y. Gu, N. A. Goodman, F. Qu, Source estimation using coprime array: A sparse reconstruction perspective, IEEE Sensors Journal 17 (3) (2017) 755–765 (Feb 2017). doi:10.1109/JSEN.2016.2637059.

[16] C. Liu, P. P. Vaidyanathan, Hourglass arrays and other novel 2-d sparse arrays with reduced mutual coupling, IEEE Transactions on Signal Processing 65 (13) (2017) 3369–3383 (July 2017). doi:10.1109/TSP.2017.2690390.
[17] J. Shi, G. Hu, X. Zhang, H. Zhou, Generalized nested array: Optimization for degrees of freedom and mutual coupling, IEEE Communications Letters 22 (6) (2018) 1208–1211 (June 2018). doi:10.1109/LCOMM.2018.2821672.
[18] C. Liu, P. P. Vaidyanathan, Super nested arrays: Linear sparse arrays with reduced mutual couplingpart I: Fundamentals, IEEE Transactions on Signal Processing 64 (15) (2016) 3997–4012 (Aug 2016). doi:10.1109/TSP.2016.2558159.
[19] C. Liu, P. P. Vaidyanathan, Super nested arrays: Linear sparse arrays with reduced mutual couplingpart II: High-order extensions, IEEE Transactions on Signal Processing 64 (16) (2016) 4203–4217 (Aug 2016). doi:10.1109/TSP.2016.2558167.
[20] J. Liu, Y. Zhang, Y. Lu, S. Ren, S. Cao, Augmented nested arrays with enhanced DOF and reduced mutual coupling, IEEE Transactions on Signal Processing 65 (21) (2017) 5549–5563 (Nov 2017). doi:10.1109/TSP.2017.2736493.
[21] A. Raza, W. Liu, Q. Shen, Thinned coprime array for second-order difference co-array generation with reduced mutual coupling, IEEE Transactions on Signal Processing 67 (8) (2019) 2052–2065 (April 2019). doi:10.1109/TSP.2019.2901380.
[22] P. Pal, P. P. Vaidyanathan, Coprime sampling and the MUSIC algorithm, in: 2011 Digital Signal Processing and Signal Processing Education Meeting (DSP/SPE), 2011, pp. 289–294 (Jan 2011). doi:10.1109/DSP-SPE.2011.5739227.
[23] R. Schmidt, Multiple emitter location and signal parameter estimation, IEEE transactions on antennas and propagation 34 (3) (1986) 276–280 (1986).
[24] S. Qin, Y. D. Zhang, M. G. Amin, Generalized coprime array configurations for direction-of-arrival estimation, IEEE Transactions on Signal Processing 63 (6) (2015) 1377–1390 (March 2015). doi:10.1109/TSP.2015.2393838.
[25] X. Wang, X. Wang, Hole identification and filling in k-times extended co-prime arrays for highly efficient DOA estimation, IEEE Transactions on Signal Processing 67 (10) (2019) 2693–2706 (May 2019). doi:10.1109/TSP.2019.2899292.
[26] W. Wang, S. Ren, Z. Chen, Unified coprime array with multi-period subarrays for direction-of-arrival estimation, Digital Signal Processing 74 (2018) 30–42 (2018).
[27] A. Ahmed, Y. D. Zhang, J. Zhang, Coprime array design with minimum lag redundancy, in: ICASSP 2019 - 2019 IEEE International Conference on Acoustics, Speech and Signal Processing (ICASSP), 2019, pp. 4125–4129 (May 2019). doi:10.1109/ICASSP.2019.8683315.
[28] J. Ramirez Jr, J. L. Krolik, Synthetic aperture processing for passive co-prime linear sensor arrays, Digital Signal Processing 61 (2017) 62–75 (2017).
[29] G. Qin, M. G. Amin, Y. D. Zhang, DOA estimation exploiting sparse array motions, IEEE Transactions on Signal Processing 67 (11) (2019) 3013–3027 (June 2019). doi:10.1109/TSP.2019.2911261.
[30] E. BouDaher, Y. Jia, F. Ahmad, M. G. Amin, Multi-frequency co-prime arrays for high-resolution direction-of-arrival estimation, IEEE Transactions on Signal Processing 63 (14) (2015) 3797–3808 (July 2015). doi:10.1109/TSP.2015.2432734.
[31] C. Liu, P. P. Vaidyanathan, P. Pal, Coprime coarray interpolation for DOA estimation via nuclear norm minimization, in: 2016 IEEE International Symposium on Circuits and Systems (ISCAS), 2016, pp. 2639–2642 (May 2016). doi:10.1109/ISCAS.2016.7539135.
[32] C. Zhou, Y. Gu, X. Fan, Z. Shi, G. Mao, Y. D. Zhang, Direction-of-arrival estimation for coprime array via virtual array interpolation, IEEE Transactions on Signal Processing 66 (22) (2018) 5956–5971 (Nov 2018). doi:10.1109/TSP.2018.2872012.
[33] T. Chen, M. Guo, L. Guo, A direct coarray interpolation approach for direction finding, Sensors 17 (9) (2017) 2149 (2017).
[34] H. Qiao, P. Pal, Gridless line spectrum estimation and low-rank Toeplitz matrix compression using structured samplers: A regularization-free approach, IEEE Transactions on Signal Processing 65 (9) (2017) 2221–2236 (May 2017). doi:10.1109/TSP.2017.2659644.
[35] A. Raza, W. Liu, Q. Shen, Thinned coprime arrays for DOA estimation, in: 2017 25th European Signal Processing Conference (EUSIPCO), 2017, pp. 395–399 (Aug 2017). doi:10.23919/EUSIPCO.2017.8081236.
[36] Z. Fu, P. Chargé, Y. Wang, Multi-rate coprime sampling for frequency estimation with increased degrees of freedom, Signal Processing 166, 107258 (2020).
[37] T. Svantesson, Mutual coupling compensation using subspace fitting, in: Proceedings of the 2000 IEEE Sensor Array and Multichannel Signal Processing Workshop. SAM 2000 (Cat. No.00EX410), 2000, pp. 494–498 (March 2000). doi:10.1109/SAM.2000.878058.
[38] E. BouDaher, F. Ahmad, M. Amin, A. Hoorfar, DOA estimation with co-prime arrays in the presence of mutual coupling, in: 2015 23rd European Signal Processing Conference (EUSIPCO), 2015, pp. 2830–2834 (Aug 2015). doi:10.1109/EUSIPCO.2015.7362901.
[39] B. Friedlander, A. J. Weiss, Direction finding in the presence of mutual coupling, IEEE Transactions on Antennas and Propagation 39 (3) (1991) 273–284 (March 1991). doi:10.1109/8.76322.
[40] Y. D. Zhang, M. G. Amin, B. Himed, Sparsity-based DOA estimation using co-prime arrays, in: 2013 IEEE International Conference on Acoustics, Speech and Signal Processing, 2013, pp. 3967–3971 (May 2013). doi:10.1109/ICASSP.2013.6638403.
[41] Q. Shen, W. Liu, W. Cui, S. Wu, Extension of co-prime arrays based on the fourth-order difference co-array concept, IEEE Signal Processing Letters 23 (5) (2016) 615–619 (May 2016). doi:10.1109/LSP.2016.2539324.